buildings

MDPI

Article

Complete Ensemble Empirical Mode Decomposition and Wavelet Algorithm Denoising Method for Bridge Monitoring Signals

Bing-Chen Yang [1], Fang-Zhou Xu [1], Yu Zhao [1], Tian-Yun Yao [2,3,*], Hai-Yang Hu [1], Meng-Yi Jia [1], Yong-Jun Zhou [1] and Ming-Zhu Li [4]

[1] School of Highway, Chang'an University, Xi'an 710064, China; 2022121085@chd.edu.cn (B.-C.Y.); a112320@126.com (F.-Z.X.); zhaoyu@chd.edu.cn (Y.Z.); 2022121040@chd.edu.cn (H.-Y.H.); 2022121043@chd.edu.cn (M.-Y.J.); zyj@chd.edu.cn (Y.-J.Z.)
[2] School of Civil Engineering, Chang'an University, Xi'an 710061, China
[3] Xi'an Qiao Bang Engineering Inspection Co., Ltd., Xi'an 710086, China
[4] School of Architecture, Xi'an University of Architecture and Technology, Xi'an 710055, China; limingzhu@xauat.edu.cn
* Correspondence: yao_yao2021@chd.edu.cn; Tel.: +86-181-0781-7777

Abstract: In order to investigate the analysis and processing methods for nonstationary signals generated in bridge health monitoring systems, this study combines the advantages of complete ensemble empirical mode decomposition (CEEMD) and wavelet threshold denoising algorithms to construct the CEEMD–wavelet threshold denoising algorithm. The algorithm follows the following steps: first, add noise to the monitoring data and obtain all the mode components through empirical mode decomposition (EMD), denoise the mode components with noise using the wavelet threshold function to remove the noise components, select the optimal stratification for denoising the monitoring data of the Guozigou Bridge in Xinjiang in January 2023, determine the wavelet type and threshold selection criteria, and reconstruct the denoised intrinsic mode function (IMF) components to achieve accurate extraction of the effective signal. By referencing the deflection, temperature, and strain data of the Guozigou Bridge in Xinjiang in January 2023 and comparing the data cleaned by different mode decomposition and wavelet threshold denoising methods, the results show that compared with empirical mode decomposition (EMD)–wavelet threshold denoising and variational mode decomposition (VMD)–wavelet threshold denoising, the signal-to-noise ratios and root-mean-square errors of the four types of monitoring data obtained by the algorithm proposed in this study are the most ideal. Under the premise of minimizing reconstruction errors when processing a large amount of data, it has better convergence, verifying the practicality and reliability of the algorithm in the field of bridge health monitoring data cleaning and providing a certain reference value for further research in the field of signal processing. The computational method constructed in this study will provide theoretical support for data cleaning and analysis of nonstationary and nonlinear random signals, which is conducive to further promoting the improvement of bridge health monitoring systems.

Keywords: bridge engineering; monitoring data; numerical calculation; complete ensemble empirical mode decomposition; wavelet threshold

Citation: Yang, B.-C.; Xu, F.-Z.; Zhao, Y.; Yao, T.-Y.; Hu, H.-Y.; Jia, M.-Y.; Zhou, Y.-J.; Li, M.-Z. Complete Ensemble Empirical Mode Decomposition and Wavelet Algorithm Denoising Method for Bridge Monitoring Signals. *Buildings* **2024**, *14*, 2056. https://doi.org/10.3390/buildings14072056

Academic Editor: Fabrizio Gara

Received: 7 June 2024
Revised: 29 June 2024
Accepted: 4 July 2024
Published: 5 July 2024

1. Introduction

The "Implementation Plan for the Construction of Structural Health Monitoring System for Long Highway Bridges" issued by the Ministry of Highway and Transport of the People's Republic of China lists 11 bridges across the country as pilot projects for the construction of structural health monitoring system and includes 401 highway long bridges across the country in the scope of real-time health monitoring, requiring real-time monitoring of the structural health of long bridges across rivers, seas, and valleys. A dynamic

grasp of the operation status of long-span bridge structures focuses on preventing and resolving major safety risks in the operation of long-span highway bridges and further improving the monitoring and safety guarantee capabilities of highway bridges. During the operation of the bridge health monitoring system, a variety of different kinds of raw data will be generated. Due to the influence of environmental factors or the system itself, a large amount of distorted data will appear in these raw data, which will have a great impact on the real-time analysis of the bridge condition. Therefore, it is of great significance to conduct cleaning research on the original monitoring data [1–3]. In the process of big data acquisition and import, a deviation or error between the measured and real values is easy to occur. These abnormal data are called noise data, and the data containing noise will affect the quality of the data and the prediction and analysis of bridge maintenance to different degrees. For the noise data of bridge health monitoring, the denoising methods commonly used at present are as follows: wavelet transform (WT), empirical mode decomposition (EMD), variational mode decomposition (VMD), complete ensemble empirical mode decomposition (CEEMD), complete ensemble empirical adaptive mode decomposition with noise (CEEMDAN), etc. [4–6]. In order to explore more effective monitoring data denoising methods, many scholars have carried out a series of studies.

Luo [7] introduced empirical wavelet transform into bridge monitoring signal noise reduction, and combined with practical engineering application requirements, he proposed a bridge structural response adaptive noise reduction method based on noise-assisted analysis theory to achieve noise reduction of bridge monitoring signals under complex environment excitation. Based on the principle of EMD and wavelet noise reduction, Shi [8] proposed an EMD–wavelet adaptive run value function noise reduction method to reduce the background noise of a full waveform three-dimensional laser mapping radar (light detection and ranging—LiDAR) in a digital topographic survey. Wang [9] proposed a digital filter denoising method based on wavelet transform combined with empirical mode decomposition to denoise low-concentration second-harmonic signals collected by tunable diode laser absorption spectroscopy. Xiong [10] proposed a combined CEEMDAN–WT denoising method to reduce GNSS-RTK monitoring signals of bridges. Paroli [11] proposed a frequency-dependent threshold method for denoising seismic maps using the S transform. The test results in this article indicate that this method performs better than traditional band-pass methods and can be used well even in situations with low signal-to-noise ratios. Rocco [12] proposed a band variable filter based on the nonlinear changes in the corresponding characteristics of soil and buildings under transient forcing in order to accurately evaluate the damage mechanism of the two under transient forcing and more accurately locate the damage on the structure. Mo [13] used a data processing method based on CEEMDAN and an adaptive threshold wavelet filtering method composed of the mean and variance of wavelet coefficients in each layer to denoise BDS displacement monitoring data. The results showed that the proposed method can effectively suppress random noise and multipath noise and effectively obtain the true response of a bridge displacement. Chen [14] used the wavelet packet energy rate index (WPERI) as a new metric for detecting cracks in curved bridge sections of rivers and found that the WPERI exhibited a nonlinear response related to an increase in crack severity, indicating its sensitivity to changes in damage strength. Jian [15] utilized the dynamic response of a tractor-trailer vehicle model to identify the bridge modal shape. Subsequently, wavelet analysis was employed to iteratively determine the bridge modal shape from the subtracted accelerations of adjacent trailers. The findings indicate that employing the wavelet denoising algorithm enhances the accuracy of identification, especially in the presence of measurement noise. Zhang [16] introduced an intelligent damage detection method for steel–concrete composite beams, which leverages deep learning and wavelet analysis and is built upon ResNet-50. The results indicate that wavelet denoising enhanced the prediction accuracy of ResNet-50 by 1.18%, thereby improving the precision of structural damage identification. Zhang [17] proposed an optimal wavelet basis design principle based on the minimum Shannon entropy, with regard to wavelet ridges and wavelet skeletons. Taking large-span cable-stayed

bridges and large-span suspension bridges as engineering backgrounds, the improved continuous wavelet transform (CWT) was applied to modal parameter identification of bridges under environmental excitation, verifying the reliability of CWT in identifying modal parameters of large-span bridges under environmental excitation.

In summary, the research on the algorithm combining modal decomposition and wavelet threshold for monitoring data in various fields has been widely carried out, but the research on the processing of nonstationary and complex signals in bridge monitoring systems is still incomplete. The combined methods of various denoising algorithms have the following shortcomings: the method combining EDM and WT has good temporal localization characteristics [18–20], but in practice, the most suitable decomposition scale [21] needs to be found to achieve the best noise reduction effect. The limitations of VMD technology mainly lie in the processing of burst signals and signals with large amounts of data [22,23]. Combined with WT, mode aliasing can be avoided more effectively [24], but it has great limitations in the processing of complex signals [25]. This paper aims to study the analysis and processing methods of nonstationary noise signals generated in a bridge health monitoring system. Combining the advantages of CEEMD and wavelet threshold methods in data processing, a CEEMD–wavelet threshold denoising algorithm is proposed to clean the real-time data of bridge health monitoring. This algorithm is used to clean the temperature, deflection, and strain data of Guozigou Bridge in Xinjiang and to accurately evaluate the service status of the bridge.

2. CEEMD–Wavelet Threshold Denoising Method Principle

2.1. Wavelet Denoising Method

Compared with the Fourier transform, the wavelet transform has higher efficiency in denoising data signals. Based on the short-time Fourier transform, wavelet transform not only has the advantage of localization but also has the characteristic that the time–frequency window can change with the change of frequency [26]. This wavelet analysis method can subdivide time at high frequency and frequency at low frequency. It has good sensitivity and accuracy and is more suitable for stationary data signal processing. Based on this, DONOHO et al. proposed a wavelet threshold filtering method.

However, the temperature and strain data are too stable, and the wavelet threshold denoising is not obvious to the noise processing, which is too close to the actual data. Moreover, wavelet threshold denoising cannot process data containing jump points and drift, and the form of data processing is too simple. For the large amount of deflection data, the cleaning effect is not significant in the process of noise cleaning. In general, the effect of wavelet threshold denoising on nonstationary and nonlinear signals is not ideal.

2.2. Denoising Reduction Method Based on CEEMD Decomposition

CEEMD is a major improvement of the EMD method. At the same time, it borrows the idea of adding Gaussian noise to the EEMD method and cancels noise through multiple superposition and environmental monitoring management and technology to effectively solve the problem of the residual noise signal and low extraction efficiency after EMD decomposition and low decomposition efficiency of EEMD and difficult-to-remove noise. The IMF component of white noise is added to each decomposition of the CEEMD method, and the noise is reduced step by step. The noise residue in the inherent mode is less, and the reconstruction error is reduced. There is a global stop standard for each decomposition stage, and the efficiency is high.

However, CEEMD still has two problems: stray mode and residual noise.

2.3. Principle of CEEMD–Wavelet Threshold Denoising Algorithm

Wavelet threshold and CEEMD methods have advantages and disadvantages in cleaning noisy data, and they can complement each other. CEEMD method has the completeness of time–frequency addition, adding Gaussian noise and multiple superpositions and averages to offset noise, and strong application adaptability, so it can make up for

the shortcomings of wavelet basis decomposition transformation method that cannot be adaptive. The wavelet threshold method has the ability of scaling and continuous time–frequency analysis, which can avoid mode aliasing. Most of the bridge health monitoring signals are nonlinear and nonstationary signals, and the wavelet threshold denoising is not suitable, while the CEEMD processing effect is better.

Based on the above analysis, a CEEMD–wavelet threshold function noise reduction method is proposed, and its algorithm flow is shown in Figure 1.

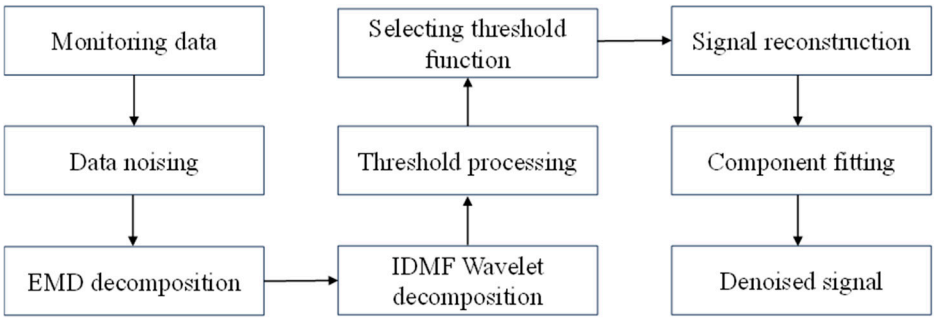

Figure 1. Process of simulation data algorithm.

① Add the data signal x to 100 groups of Gaussian white noise with a standard deviation of 0.4 to synthesize the data signal x^i with noise, that is,

$$x^i = x + \beta_k w^i \tag{1}$$

where x is the data signal, $w^i(i = 1, 2, \cdots, 100)$ is a group of Gaussian white noise whose unit variance mean is 0; β_k is the standard deviation of the added Gaussian white noise.

② The first mode is obtained by EMD calculation

$$IMF_1 = \frac{\sum_{i=1}^{m} E_1(w^i)}{m} \tag{2}$$

Then the first-order residual is

$$r_1 = x - IMF_1 \tag{3}$$

③ Calculate the second residual and the second mode

$$IMF_2 = \frac{\sum_{i=1}^{m} E_2(r_i + b_1 E_1(w^i))}{m} \tag{4}$$

$$r_2 = r_1 - IMF_2 \tag{5}$$

④ Calculate the NTH residual and the NTH mode by analogy

$$IMF_n = \frac{\sum_{i=1}^{m} E_n(r_{n-1} + \beta_{n-1} E_{n-1}(w^i))}{m} \tag{6}$$

$$r_n = r_{n-1} - IMF_n \tag{7}$$

where m is the number of noise signals added; $E_n(*)$ is the NEH order EMD component obtained through EMD decomposition.

Repeat step 4 until the residual cannot be decomposed and the full IMF is calculated.

⑤ Denoise the IMF component with noise by the wavelet threshold function as a whole, retain the remaining pure IMF component after denoising, and eliminate the noise component.

⑥ Select the optimal stratification for denoising the health monitoring data of Xinjiang Guozigou Bridge, keep other variables unchanged, and determine the wavelet type and threshold selection criteria. The calculation formula for the global threshold is as follows:

$$\delta_g = \sigma\sqrt{2\log(M \times N)} \tag{8}$$

where σ is the standard deviation of noise; M, N are the signal scale.

Select the threshold function

$$W_{\delta\ i} = \begin{cases} \tanh(W_i)[|W_i| - (1 - \exp(\frac{-K}{|W_i|-\delta_i}))\delta_i], |W_i| \geq \delta_i \\ \tanh(W_i)[|W_i| - \frac{\delta_i}{\exp{(|W_i|-\delta_i)^m T}}], |W_i| < \delta_i \end{cases} \tag{9}$$

where W_i is the coefficient corresponding to the i layer of the wavelet transform; T is the compression factor, and its default value is 1; δ_i is the threshold corresponding to layer i in the wavelet transform.

⑦ Reconstruct the IMF component after denoising to achieve accurate extraction of effective signals.

3. Project Overview and Measuring Point Layout

3.1. Project Overview

Xinjiang Guozigou Bridge is a steel girder cable-stayed bridge with two towers and two cable planes. The main beam is provided with longitudinal movement and vertical rigidity spherical supports, and each main tower is provided with four transverse wind supports, and a group of hydraulic dampers is provided at each main girder, each side pier, and the two beams in the main tower, with a total of eight sets. The main tower is a stepped reinforced concrete structure, and the column is a single box and single chamber section, made of C50 concrete. The cable-stayed cable is a double-plane fan-shaped arrangement, which adopts PES (FD) new low-stress anticorrosion cable and uses double HDPE for protection. High-strength steel wire is manufactured using Φ7 galvanized steel, with a standard tensile strength of 1670 MPa. In the design of steel truss beam, the structure form of the "N" truss is adopted. This structure form is composed of two main trusses. In order to increase the stability of the main trusses, the welded integral joint structure is adopted. At the same time, the upper and lower chords use a box section, and a plate stiffener is arranged on each side of the vertical plate. The vertical and oblique rods of the main girder are "H"-shaped sections, and the maximum lifting weight can reach 17 tons.

At the functional level, the importance of the Guozigou Bridge is self-evident during the operation of the core traffic hub of the G30 high-speed trunk line. At present, the surrounding roads have not been built to share the current traffic flow. If the bridge is seriously damaged, it will cause great inconvenience and have a negative impact on the traffic. Therefore, the health monitoring of this bridge is very important.

3.2. Measuring Point Layout

(1) Load source monitoring

In order to ensure the durability of steel components, temperature and humidity monitoring equipment in the middle of the main span and in the anchoring area of the cable tower is mainly used for temperature and humidity monitoring. Its main purpose is to monitor the digital indexes of air temperature and humidity at the main beam and assist in monitoring the maintenance of the main beam of the steel structure of the bridge. At the same time, temperature and humidity monitoring equipment is also an important parameter standard for analyzing the development state of structural changes and structural damage. The location and number of measuring points are shown in Figure 2 and Table 1.

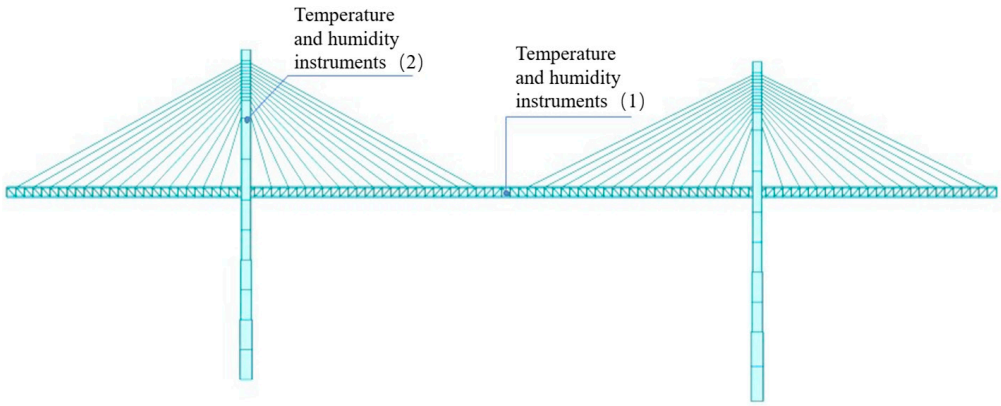

Figure 2. Schematic layout of temperature and humidity measuring points.

The temperature and humidity instruments utilized at the monitoring point are shown in Figure 3.

Figure 3. The temperature and humidity instrument.

Table 1. Location and quantity of temperature and humidity detectors.

Location	Number of Measurement Points	Measurement Frequency	Sensor Type
Z1 tower anchor zone Mid span of the main span	2 1	Once/10 min	Temperature and humidity instruments

(2) Deflection of the main beam

The deflection of the main beam is monitored by the bridge deformation dynamic monitoring system. The multipoint dynamic deformation long-term monitoring system of the bridge is based on the image principle, which is developed in view of the shortcomings of the current bridge deformation monitoring. The instrument is part of the professional monitoring equipment with long-distance measurement ability, high precision, stable measurement value, strong anti-environmental interference performance, and multipoint real-time dynamic deformation. The location and quantity of measuring points are shown in Figure 4 and Table 2.

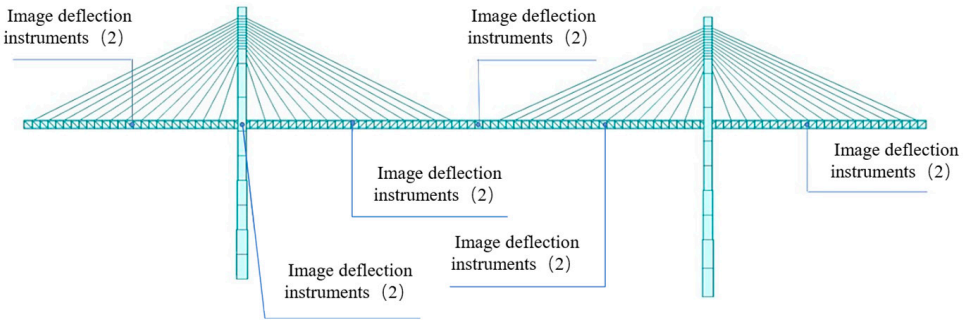

Figure 4. Deflection measuring points of the main beam.

The image deflection instruments utilized at the monitoring point are shown in Figure 5.

Figure 5. The image deflection instrument.

Table 2. Location and number of deflection meters in the image.

Location	Number of Measurement Points	Measurement Frequency	Sensor Type
Kuitun side span	2	10 Hz~300 Hz	Image deflection instruments
Z1 tower beam junction	2		
Z1 tower beam junction	2		
Mid span of the main span	2		

(3) Structural stress

Stress monitoring is one of the core functions of intelligent bridge monitoring, which is directly related to the safety of the structure. By comparing with the theoretical value, parameter estimation, prediction, and modification of the measured value are carried out, which is an important basis for ensuring the safe operation of the bridge. By monitoring the stress of the bridge girder, we can know the stress condition of the bridge deck under external load, including traffic load and natural load. By analyzing the amplitude of stress variation, the stress variation of the member is monitored, which provides theoretical guidance for structural safety evaluation. A vibration string strain gauge is used for strain monitoring. The specific location and quantity are shown in Figure 6 and Table 3.

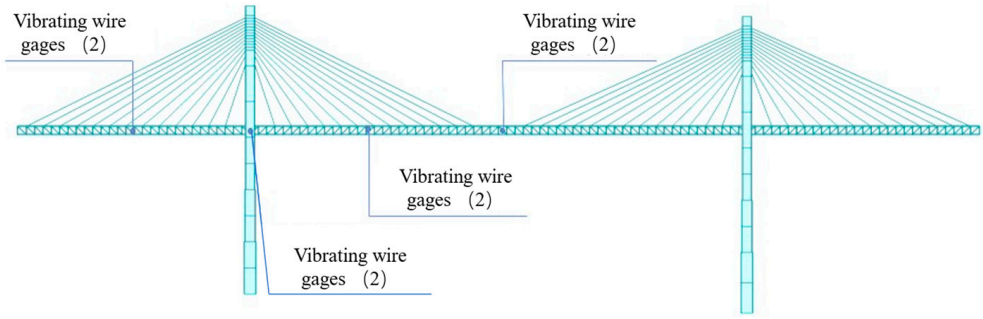

Figure 6. Layout of measuring points of strain gauges.

The vibrating wire gages utilized at the monitoring point are shown in Figure 7.

Figure 7. The vibrating wire gage.

Table 3. Location and quantity of strain gauges.

Location	Number of Measurement Points	Measurement Frequency	Sensor Type
Mid span of Kuitun side span	12	Once/10 min	Vibrating wire gages
The main beam at the junction of tower and beam	12		
Main beam at L/4 of the main span	12		
Mid span of the main span	12		

4. Results and Discussion

4.1. Evaluation Indicators

When evaluating the effect of noise removal, two indicators are usually used: the signal-to-noise ratio (SNR) and root-mean-square error (RMSE).

(1) Signal-to-Noise Ratio

The signal-to-noise ratio is used as the standard rule to evaluate the effectiveness of signal denoising. SNR is the ratio of the energy difference between the original signal and the denoised signal. The larger the SNR value, the smaller the proportion of the noise component in the signal and the better the denoising effect. The formula is

$$SNR = 10 \times \log_{10}\left[\frac{Q_s}{Q_n}\right] \tag{10}$$

$$Q_s = \frac{1}{M}\sum_{t=1}^{M}\left[Q(t) - \hat{Q}(t)\right]^2 \tag{11}$$

$$Q_n = \frac{1}{M}\sum_{t=1}^{1}\left[Q(t) - \hat{Q}(t)\right]^2 \tag{12}$$

where Q_s is the power of the original signal; Q_n is the component of noise in the original signal; $S(t)$ Is the original signal; $\hat{S}(t)$ is the decomposed reconstructed signal after decomposing and denoising; M is the signal length.

(2) Root-Mean-Square Error

The root-mean-square error represents the error between the observed value and the real value, reflecting the similarity between the original signal and the denoised reconstructed signal, and can be used as an evaluation index of the degree of deviation between the denoised reconstructed signal and the original signal. The smaller the RMSE, the higher the degree of similarity between the signal and the better the degree of restoration. Its calculation formula is as follows:

$$R(X,h) = \sqrt{\frac{1}{m}\sum_{i=1}^{m}\left(h(x_i) - y_i\right)^2} \tag{13}$$

where $R(X,h)$ is the root-mean-square error; m is the number of samples; y_i is the true value of the original signal; $h(x_i)$ is the observed value of the noise reduction signal corresponding to the original signal.

4.2. Strain Cleaning Results

In the process of strain data analysis of the Guozigou Bridge in Xinjiang, 100 groups of Gaussian white noise with a standard deviation of 0.4 are added to the original signal for CEEMD decomposition. The center frequency of each fraction is as follows: IMF1 = 0.5017, IMF2 = 0.1149, IMF3 = 0.1010, IMF4 = 0.0662, IMF5 = 0.0313, IMF6 = 0.0104, IMF7 = 0.0034, and res = 0. The retained components of IMF2, IMF3, IMF4, IMF5, IMF6, IMF7, and res are denoised by wavelet threshold, and the best fitting results are selected.

For the processing of strain data from the Guozigou Bridge in Xinjiang, this paper uses the CEEMD–wavelet threshold method to denoise and carry out component fitting. Equations (10) and (13) are utilized to compute the signal-to-noise ratio and root mean square error of the fitted data. The results show that the signal-to-noise ratio after denoising reaches 35.089. The root-mean-square error is 9.076. The comparison between the strain noise reduction and the original data is shown in Figure 8. Although there are differences in local details, overall, the data change trend after denoising is basically the same and within a reasonable range.

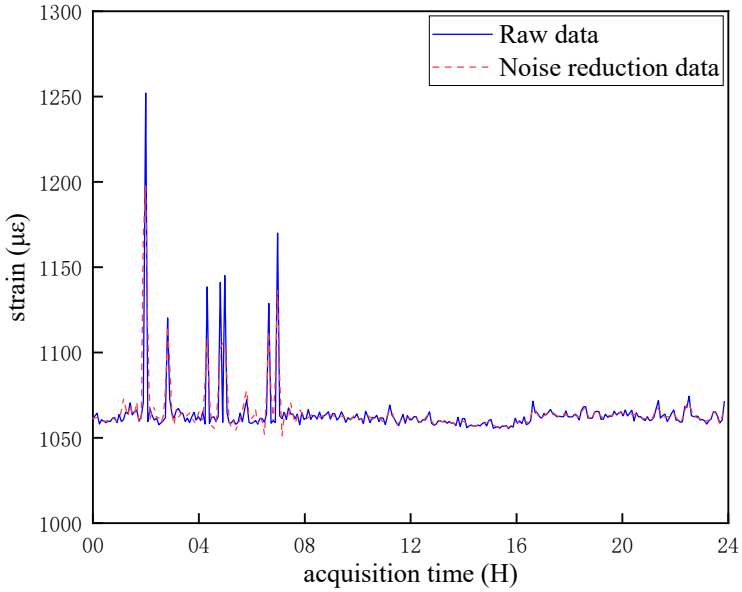

Figure 8. Strain data noise cleaning.

The denoising effect of the strain mode decomposition function is shown in Table 4.

Table 4. Comparison table of strain mode decomposition and noise reduction data.

Function Type	SNR	RMSR
EMD wavelet threshold denoising	27.813	15.234
VMD wavelet threshold denoising	31.471	13.397
CEEMD wavelet threshold denoising	35.089	9.076

The results show that the signal-to-noise ratio after denoising is 35.089 and the root-mean-square error is 9.0776.

4.3. Temperature Cleaning Result

When analyzing the temperature data from the Guozigou Bridge in Xinjiang, 100 groups of Gaussian white noise with a standard deviation of 0.4 are added to the temperature signal collected by the sensor to simulate the noise environment. The temperature signal after adding noise is decomposed by CEEMD. The center frequency of each component decomposition is as follows: IMF1 = 0.2648, IMF2 = 0.1777, IMF3 = 0.0941, IMF4 = 0.0418, IMF5 = 0.0243, IMF6 = 0.0069, IMF7 = 0.0068, and res = 0. The IMF2, IMF3, IMF4, IMF5, IMF6, IMF7, and res components are retained and wavelet threshold denoising is carried out to select the best fitting results.

For the processing of the temperature data from the Guozigou Bridge in Xinjiang, this paper uses the CEEMD–wavelet threshold method to reduce noise and carry out component fitting. Equations (10) and (13) are utilized to compute the signal-to-noise ratio and root mean square error of the fitted data. The results show that the signal-to-noise ratio after denoising is 31.640, and the root-mean-square error is 0.132. As shown in Figure 9, the change trend of the data after denoising is basically the same as that of the original data. After adding complementary white noise to the temperature data and neutralizing it, the results show that the data reconstruction error after noise reduction is relatively small, and the frequency distribution is more suitable. These processes help reduce the distortion rate of the temperature data in the bridge health monitoring system.

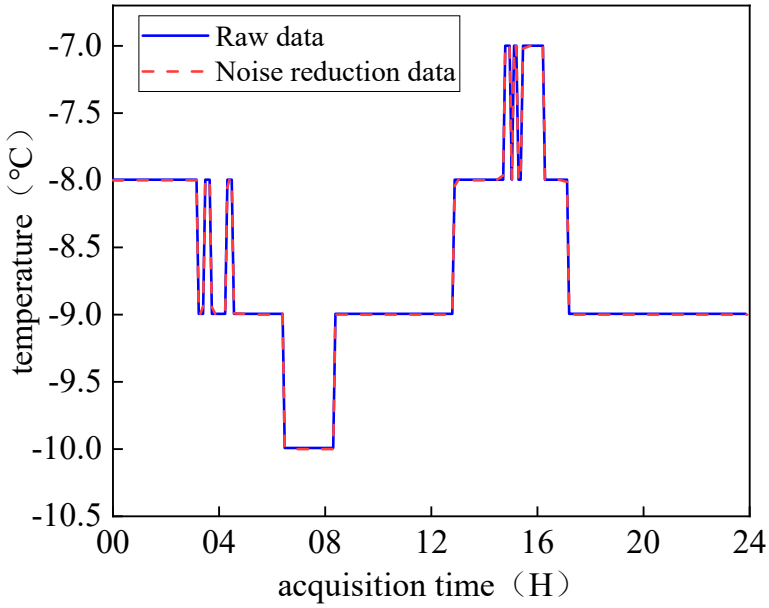

Figure 9. Temperature data noise cleaning.

The denoising effect of the temperature modal decomposition function is shown in Table 5.

Table 5. Comparison table of temperature modal decomposition and noise reduction data.

Function Type	SNR	RMSR (°C)
EMD wavelet threshold denoising	20.963	0.5936
VMD wavelet threshold denoising	29.966	0.173
CEEMD wavelet threshold denoising	31.640	0.132

The results show that the signal-to-noise ratio after denoising is 31.640 and the root-mean-square error is 0.132.

4.4. Deflection Cleaning Results

When analyzing the deflection data from the Guozigou Bridge in Xinjiang, 100 groups of Gaussian white noise with a standard deviation of 0.4 are added to the deflection signals collected by sensors to simulate the noise environment. The deflection signal after noise is decomposed by CEEMD. The central frequencies of each component are as follows: IMF1 = 0.4019, IMF2 = 0.1407, IMF3 = 0.1007, IMF4 = 0.0428, IMF5 = 0.0269, IMF6 = 0.0113, IMF7 = 0.0018, IMF8 = 0.0018, IMF9 = 0.0009, IMF10 = 0.0002, IMF11 = 0.0003, IMF12 = 0.0001, and res = 0. The IMF2, IMF3, IMF4, IMF5, IMF6, IMF7, IMF8, IMF9, IMF10, IMF11, IMF12, and res quantities are retained and denoised by wavelet threshold and the best fit results are selected.

For the deflection data from the Guozigou Bridge in Xinjiang, this paper uses the CEEMD–wavelet threshold method to denoise and carry out component fitting. Equations (10) and (13) are utilized to compute the signal-to-noise ratio and root-mean-square error of the fitted data The results show that the signal-to-noise ratio after denoising is 20.614 and the root-mean-square error is 1.330. Among them, the comparison results between the data after denoising of deflection and the original data are shown in Figure 10. It can be seen that the sample size of deflection data within 24 h is very large, and the decomposition results of EMD and VMD will be poor due to their own limitations when processing signals with large amounts of data. To this end, the CEEMD decomposition technique is introduced in this paper, and the modal effect is further reduced by adding adaptive noise when processing large amounts of

data. The research shows that this technique has better convergence on the premise of small reconstruction error when processing a large number of data.

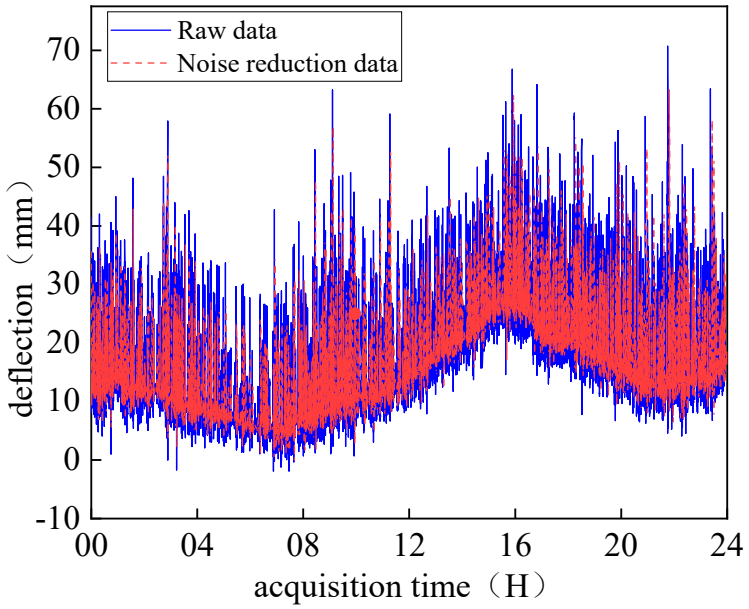

Figure 10. Deflection data noise cleaning.

The denoising effect of the deflection mode decomposition function is shown in Table 6.

Table 6. Comparison table of deflection mode decomposition and denoising data.

Function Type	SNR	RMSR (mm)
EMD wavelet threshold denoising	11.039	3.921
VMD wavelet threshold denoising	12.665	1.616
CEEMD wavelet threshold denoising	20.614	1.330

The results show that the signal-to-noise ratio after denoising is 20.614 and the root-mean-square error is 1.330.

5. Conclusions

(1) By comparing the SNR and the mean square error of temperature, deflection, and strain after EMD–wavelet threshold denoising and VMD–wavelet threshold denoising methods, it is found that the SNR of deflection after denoising by this method is 63% higher than that after VMD–wavelet threshold denoising. The mean square error of strain after denoising is 40% lower than that of the data after EMD–wavelet threshold noise reduction.

(2) This method has the advantages of a large data sample and high mode decomposition performance when dealing with nonlinear and nonstationary data, which provides a certain reference value for further research in the field of signal processing.

(3) Maintaining the integrity of the original signal while reducing noise has superior application potential.

(4) Due to constraints in the engineering environment and equipment, this study cannot precisely compare the collected data in the time–frequency domain. For future research, the synchronous squeezing wavelet transform method can be employed for high-precision data processing.

(5) All conclusions drawn in this study are specific to the project referenced and may not be applicable to all scenarios.

Author Contributions: B.-C.Y.: writing the original draft. F.-Z.X.: data curation. Y.Z.: data curation. T.-Y.Y.: writing—review and editing. H.-Y.H.: analysis. M.-Y.J.: writing original draft and software. Y.-J.Z.: data curation and software. M.-Z.L.: data curation and software. All authors have read and agreed to the published version of the manuscript.

Funding: This work was supported by the National Key Research and Development Program of China (2021YFB1600302) and the Natural Science Foundation Research Program of Shaanxi Province (2024JC-YBON-0387).

Data Availability Statement: Data are contained within the article.

Conflicts of Interest: Author Tian-Yun Yao was employed by Xi'an Qiao Bang Engineering Testing Co., Ltd. The remaining authors declare that the research was conducted in the absence of any commercial or financial relationships that could be construed as a potential conflict of interest.

References

1. Xue, G.H.; Li, M.H.; Han, Y.X. Research on multi-source data prediction algorithm for bridge structural health monitoring based on correlation analysis. *Railw. Eng.* **2022**, *62*, 73–79.
2. Editorial Department of 'China Journal of Highway and Transport. Review on China's Bridge Engineering Research: 2021. *China J. Highw. Transp.* **2021**, *34*, 197.
3. Ye, H.Y.; Zhuo, Y.; Yang, X.L. Research on wavelet packet denoising of tunnel blasting vibration signals after EEMD decomposition. *Railw. Eng.* **2019**, *59*, 59–63.
4. Liu, X.Y.; Shan, D.S.; Tan, K.X. Near field pulse seismic signal denoising algorithm based on complementary set empirical mode decomposition. *Railw. Eng.* **2019**, *59*, 59–63.
5. Ma, J.; Li, H.; Chen, Y.; Wang, J.; Zou, Z. Application of VMD and dynamic wavelet noise reduction techniques in rolling bearing fault diagnosis. *Phys. Conf. Ser.* **2023**, *2528*, 012048. [CrossRef]
6. Tiziano, P.; Francesco, G.; Francesco, S. Proper orthogonal decomposition, dynamic mode decomposition, wavelet and cross wavelet analysis of a sloshing flow. *Fluids Struct.* **2022**, *112*, 103603.
7. Luo, Y.K.; Chen, Y.G.; Li, S.C. Adaptive denoising method of bridge vibration signal based on EWT-noise aided analysis theory. *Vib. Shock* **2022**, *41*, 246–256.
8. Shi, Z.Y.; Xu, W.M.; Zhou, B. A self-adapting denoising method based on empirical mode decomposition and wavelet threshold. *Hydrogr. Surv. Charting* **2021**, *41*, 54–57+72.
9. Wang, J.; Zhang, L.F.; Yang, J.S. Noise reduction of wavelength-modulated signal based on wavelet and empirical mode decomposition. *Laser Optoelectron. Progress.* **2022**, *59*, 481–487.
10. Xiong, C.B.; Wang, M.; Yu, L.N. CEEMDAN-WT joint denoising method for bridge GNSS-RTK deformation monitoring data. *Vib. Shock* **2021**, *40*, 12–18.
11. Stefano, P. Denoising of seismograms using the S transform. *Bull. Seismol. Soc. Am.* **2009**, *99*, 226–234.
12. Ditommaso, R.; Mucciarelli, M.; Ponzo, F.C. Analysis of non-stationary structural systems by using a band-variable filter. *Bull. Earthq. Eng.* **2012**, *10*, 895–911. [CrossRef]
13. Mo, C.; Yang, H.; Xiang, G.; Wang, G.; Wang, W.; Liu, X.; Zhou, Z. Displacement monitoring of a bridge based on BDS measurement by CEEMDAN–adaptive threshold wavelet method. *Sensors* **2023**, *23*, 4268. [CrossRef] [PubMed]
14. Chen, L.; Lu, X.; Deng, D.; Kouhdarag, M.; Mao, Y. Optimized wavelet and wavelet packet transform techniques for assessing crack behavior in curved segments of arched beam bridges spanning rivers. *Water* **2023**, *15*, 3977. [CrossRef]
15. Jian, X.D.; Ye, X.; Sun, L. An indirect method for bridge mode shapes identification based on wavelet analysis. *Struct. Control. Health Monit.* **2020**, *27*, 2630. [CrossRef]
16. Zhang, C.P.; Shi, J.F.; Huang, C.P. Identification of damage in steel—concrete composite beams based on wavelet analysis and deep learning. *Struct. Durab. Health Monit.* **2024**, *18*. [CrossRef]
17. Zhang, M.J.; Huang, X.; Li, Y.L.; Sun, H.; Zhang, J.Y.; Huang, B. Improved Continuous Wavelet Transform for Modal Parameter Identification of Long-Span Bridges. *Shock. Vib.* **2020**, *2020*, 4360184. [CrossRef]
18. Luo, P.; Chen, J.Y.; Guo, L.J. Study on de-noising of signal of power station based on empirical mode decomposition and modified wavelet soft threshold de-noising method. *Mech. Eng.* **2023**, *45*, 736–743.
19. Ladrova, M.; Sidikova, M.; Martinek, R. Elimination of Interference in Phonocardiogram Signal Based on Wavelet Transform and Empirical Mode Decomposition. *IFAC Pap. Online* **2019**, *52*, 440–445. [CrossRef]
20. Zhang, J.J. Magnetic Flux Leakage Image Enhancement Using Bidimensional Empirical Mode Decomposition with Wavelet Transform Method in Oil Pipeline Nondestructive Evaluation. *J. Magn.* **2019**, *24*, 423–428.
21. Xue, Z.H.; Li, G.Y.; Zhou, R. A signal denoising method based on empirical mode decomposition. *Surv. Mapp. Bull.* **2012**, 7–9.
22. Lin, J.L.; Zheng, J.Y.; Lin, Y.Q. Instantaneous frequency identification of time-varying structures using variational mode decomposition and synchrosqueezing wavelet transform. *Vib. Shock.* **2018**, *37*, 24–31.
23. Zhang, R.L.; Tu, X.H. Variational mode decomposition and wavelet threshold function de-noising for second harmonics. *Acta Opt. Sin.* **2022**, *42*, 80–87.

24. Yang, L.; Feiyun, X. Structural Damage Monitoring for Metallic Panels Based on Acoustic Emission and Adaptive Improvement Variational Mode Decomposition–Wavelet Packet Transform. *Struct. Health Monit.* **2022**, *21*, 710–730.
25. Luo, Y.Y.; Huang, C.; Zhang, J.Y. Denoising method of deformation monitoring data based on variational mode decomposition. *Geomat. Inf. Sci. Wuhan Univ.* **2020**, *45*, 784–790.
26. Jiang, T.Y.; Yu, C.Y.; Huang, K. Bridge signal denoising method combined VMD parameters optimized by aquila optimizer with wavelet threshold. *China J. Highw. Transp.* **2023**, *36*, 158–168.